Atmos. Meas. Tech. Discuss., 4, 4753–4800, 2011
www.atmos-meas-tech-discuss.net/4/4753/2011/
doi:10.5194/amtd-4-4753-2011

Atmospheric Measurement Techniques Discussions

Validation of SCIAMACHY limb NO_2 profiles using solar occultation measurements

R. Bauer[1], A. Rozanov[1], C. A. McLinden[2], L. L. Gordley[3], W. Lotz[1], J. M. Russell III[4], K. A. Walker[5], J. M. Zawodny[6], A. Ladstätter-Weißenmayer[1], H. Bovensmann[1], and J. P. Burrows[1]

[1]Institute of Environmental Physics (IUP), University of Bremen, Bremen, Germany
[2]Air Quality Research Division, Environment Canada, Toronto, Ontario, Canada
[3]GATS, Inc., Newport News, Virginia, USA
[4]Center for Atmospheric Sciences, Hampton University, Hampton, Virginia, USA
[5]Department of Physics, University of Toronto, Toronto, Ontario, Canada
[6]NASA Langley Research Center, Hampton, Virginia, USA

Received: 20 July 2011 – Accepted: 22 July 2011 – Published: 28 July 2011

Correspondence to: R. Bauer (ralf.bauer@iup.physik.uni-bremen.de)

Published by Copernicus Publications on behalf of the European Geosciences Union.

Abstract

The increasing amounts of reactive nitrogen in the stratosphere necessitates accurate global measurements of stratospheric nitrogen dioxide (NO_2). Over the past decade, the SCIAMACHY (SCanning Imaging Absorption spectroMeter for Atmospheric CHartographY) instrument on ENVISAT (European Environmental Satellite) has been providing global coverage of stratospheric NO_2 every 6 days, which is otherwise difficult to achieve with other systems (e.g. balloon measurements, solar occultation). In this study, the vertical distributions of NO_2 retrieved from limb measurements of the scattered solar light from the SCIAMACHY instrument are validated using NO_2 products from three different satellite instruments (SAGE II, HALOE and ACE-FTS). The retrieval approach, as well as the sensitivity of the SCIAMACHY NO_2 limb data product are discussed, and the photochemical corrections needed to make this validation feasible, as well as the chosen collocation criteria are described. For each instrument, a time period of two years is analyzed with several hundreds of collocation pairs for each year and instrument. The agreement between SCIAMACHY and each instrument is found to be better than 10 % between 22–24 km and 40 km. Additionally, NO_2 amounts in three different latitude regions are validated individually, with considerably better agreements in high and middle latitudes compared to tropics. Differences with SAGE II and ACE-FTS below 20 km are consistent with those expected from the diurnal effect.

1 Introduction

As a minor constituent of the atmosphere, NO_2 is known for its influence on ozone concentrations. NO_x is responsible for up to 70 % of the ozone loss in the stratosphere, see Crutzen (1970); Portmann et al. (1999). The NO_x reactions dominating the catalytic ozone destruction between about 25 and 40 km are:

AMTD

4, 4753–4800, 2011

$$NO + O_3 \rightarrow NO_2 + O_2 \quad (1)$$

$$NO_2 + h\nu \rightarrow NO + O \quad (2)$$

$$NO_2 + O \rightarrow NO + O_2. \quad (3)$$

While NO_2 participates in the destruction of ozone in the stratosphere, the same species leads to the formation of ozone in the troposphere globally, particularly during dense smog episodes. The major source for stratospheric NO_2 (hence, the major cause of ozone depletion) is nitrous oxide (N_2O), see Montzka et al. (2011), an important greenhouse gas. It is also the most important ozone depleting gas that is not covered by the Montreal Protocol (Ravishankara et al., 2009), while reduction of N_2O emission is part of the Kyoto Protocol. In the troposphere, other sources such as lightning events, anthropogenic emissions and biomass burning events contribute to ozone depletion.

In this work, we investigate the performance of the SCIAMACHY NO_2 scientific retrieval processor (version 3.1) developed at the Institute of Environmental Physics, Bremen. Measurements from SCIAMACHY (SCanning Imaging Absorption spectroMeter for Atmospheric CHartographY), a passive imaging spectrometer (Burrows et al., 1995; Bovensmann et al., 1999) on the European environmental satellite ENVISAT, are the basis for this investigation. The satellite instruments used for validation are the solar occultation instruments SAGE II (Stratospheric Aerosol Gas Experiment, Chu et al., 1989) on the Earth Radiation Budget Satellite (ERBS) of the NASA (National Space Agency, USA), (Halogen Occultation Experiment, Russell III et al., 1993) on the US satellite UARS (Upper Atmosphere Research Satellite), and ACE-FTS (Atmospheric Chemistry Experiment-Fourier Transform Spectrometer, Walker et al., 2005; Bernath et al., 2005) on the Canadian satellite SCISAT-1. The SCIAMACHY results discussed here are retrieved from measurements of the scattered solar light in limb geometry. While solar occultation instruments can provide NO_2 distributions with a high accuracy, the spatial coverage of occultation instruments is poor when compared to that achieved in limb. As those instruments still provide a significant number of retrieved NO_2 profiles, a large number of comparisons can be performed. Due to the strong diurnal variation of NO_2, photochemical corrections need to be applied, as described in Sect. 2.3.

The first part of this work gives a description of the SCIAMACHY limb NO_2 retrieval, its sensitivity and error sources (including pointing, aerosols, clouds and diurnal effect error), and explains the photochemical correction method needed for NO_2 validation. The second part gives a short description of the occultation satellite instruments and the collocation criteria applied in this study, followed by a detailed discussion of the results of the validation efforts.

2 SCIAMACHY limb observations

The SCIAMACHY instrument (Burrows et al., 1995; Bovensmann et al., 1999) on ENVISAT is a passive imaging spectrometer that comprises 8 spectral channels and covers a wide spectral range from 240 to 2400 nm. Each spectral channel is equipped with a grating spectrometer having a 1024 element diode array as a detector. For this study, only the measurements in spectral channel 3 ranging from 394 to 620 nm are used. This channel features a spectral resolution of 0.44 nm and a spectral sampling of 0.22 nm.

While SCIAMACHY features three viewing geometries, limb, nadir and occultation, only the limb mode is discussed here. In this mode, SCIAMACHY observes the atmosphere tangentially to the Earths surface. The measurement begins at about 3 km below the horizon with the Earth still in the field of view, and continues vertically upwards to an altitude of about 100 km. At each tangent height, a horizontal scan of the duration of 1.5 s is performed followed by an elevation step with no measurements of about 3.3 km, i.e. the vertical sampling is 3.3 km. The vertical instantaneous field of view of the SCIAMACHY instrument is about 2.5 km and the horizontal instantaneous field of view is 110 km at the tangent point. However, the horizontal resolution is mainly determined by the integration time during the horizontal scan resulting typically in a value of about 240 km.

In the 420 to 470 nm spectral range considered in this study, typical values of the signal to noise ratio in limb measurements range from 3000 to 5000 at tangent heights between 20 and 30 km, decreasing to about 900 near the normalization tangent height. For more information about SCIAMACHY noise characteristics, see Noël et al. (1998).

Throughout this study, SCIAMACHY Level 1 data version 6.03 were used applying the calibration steps from 0 to 5, i.e., the wavelength calibration was performed and the corrections for memory effect, leakage current, pixel-to-pixel gain, etalon, and internal stray light were accounted for. The polarization correction, as well as the absolute radiometric calibration was not applied as they do not impact the NO_2 retrieval.

2.1 SCIATRAN NO_2 limb retrieval

The SCIATRAN software package (Rozanov, 2011) is both a radiative transfer model and a retrieval algorithm that can be adjusted for a wide range of scientific tasks. It is used for NO_2 vertical profile retrieval from SCIAMACHY limb measurements as described below. In this study, version 3.1 of the NO_2 retrieval algorithm is used, which is based on SCIATRAN V2.2. The general retrieval setting for this version is described and the retrieval algorithm is presented.

NO2 retrieval as performed by version 3.1 of the retrieval processor works on the spectral range 420 to 470 nm and makes use of the differential absorption structure of NO_2. Also, O_3 is retrieved simultaneously, as it is the other important absorber in this spectral region, and O_4 is included in the forward model. The surface albedo is set to a standard value of 0.3. The tangent heights selected cover the range of about 10 to 40 km, while the reference tangent height is about 43 km. The signal-to-noise ratio is estimated from the spectral residuals. Pressure and temperature information is taken from the ECMWF database and the NO_2 cross section from Bogumil et al. (1999) are used. A background aerosol scenario from LOWTRAN (Kneizys et al., 2002) is also included in the forward model. A climatological data base provided by C.A. McLinden (personal communications, 2011) is the source of the a priori profiles needed for the retrieval. While not part of the NO_2 retrieval, the SCIAMACHY NO_2 product includes

AMTD

4, 4753–4800, 2011

Validation of SCIAMACHY limb NO_2 profiles

R. Bauer et al.

results from SCODA (SCIAMACHY cloud detection algorithm, Eichmann et al., 2009), see also von Savigny et al. (2005).

The general retrieval problem can be stated in this form:

$$\boldsymbol{y} = \boldsymbol{F}(\boldsymbol{x}) + \varepsilon, \tag{4}$$

where $\boldsymbol{F}$ is the non-linear forward model operator, $\boldsymbol{y}$ the data vector, $\boldsymbol{x}$ the state vector and ε represents remaining errors. $\boldsymbol{x}$ contains the atmospheric parameters to be retrieved, e.g. aerosol characteristics or molecular density profiles, like NO_2 vertical profiles. The data vector $\boldsymbol{y}$ contains the spectral information from all spectral points in the selected range for all used tangent heights and makes use of a technique similar to DOAS (Differential optical absorption spectroscopy, Platt, 1994). The reference tangent height is used as a background, i.e. the limb radiances are normalized with respect to the radiance at this tangent height. With this approach, the solar Fraunhofer structure is mostly eliminated as a problem and the instrument response function has a much smaller influence, and no absolute calibration is needed. Furthermore, the effect of the instrument degradation over the years of operation in space upon the retrieval results is minimized.

The retrieval problem (Eq. 4) can be approximated as a linear model, as follows:

$$\boldsymbol{y} = \boldsymbol{y}_0 + \mathbf{K}_0(\boldsymbol{x} - \boldsymbol{x}_0) + \varepsilon. \tag{5}$$

Here, $\boldsymbol{y}_0$ is the measurement vector corresponding to the a priori profile, $\boldsymbol{x}_0$ its state vector and $\mathbf{K}_0$ is a linear forward model operator. $\mathbf{K}_0$ is identified as

$$\boldsymbol{F}(\boldsymbol{x}) \approx \boldsymbol{F}(\boldsymbol{x}_0) + \left.\frac{\delta \boldsymbol{F}}{\delta \boldsymbol{x}}\right|_{\boldsymbol{x}_0} (\boldsymbol{x} - \boldsymbol{x}_0) = \boldsymbol{F}(\boldsymbol{x}_0) + \mathbf{K}_0(\boldsymbol{x} - \boldsymbol{x}_0) \tag{6}$$

The retrieval process is divided into two steps. One is the pre-processing step, which is performed to get rid of most spectral features not associated with retrieval parameters. At this step, measurements at different tangent heights (with the exception of the reference tangent height) are processed independently. First, a polynomial is subtracted

AMTD
4, 4753–4800, 2011
Validation of SCIAMACHY limb NO_2 profiles
R. Bauer et al.

from the logarithms of the measurement spectra at each tangent height and the reference tangent height, and from the logarithms of the simulated spectra and from the weighting functions. This is done in order to minimize the influence of broadband instrument calibration errors and unknown scattering characteristics of the atmosphere. Then, a shift and squeeze correction and scaling factors for correction spectra (in this implementation ring spectra, undersampling and stray light correction) are obtained. Correction spectra are also called pseudoabsorbers, see Sioris et al. (2003); Haley et al. (2004). The measurement data are corrected using the results from the pre-processing step.

The aim of the second step in the retrieval process is to solve the inverse problem. Computing the trace gas amounts from a set of measured spectra is far more difficult than generating spectra given a known set of trace gases and their absorption features. The radiative transfer equation describing the relation between radiance measured by the instrument and atmospheric parameter needs to be inverted.

To achieve this, the following quadratic form needs to be minimized:

$$\left\|(\boldsymbol{y}-\boldsymbol{y}_0)-\mathbf{K}_0(\boldsymbol{x}-\boldsymbol{x}_0)\right\|^2_{\mathbf{S}_\varepsilon^{-1}}+\left\|(\boldsymbol{x}-\boldsymbol{x}_0)\right\|^2_{\mathbf{R}} \tag{7}$$

In this equation, $\mathbf{S}_\varepsilon$ is the measurement error covariance matrix and $\mathbf{R}$ the regularization matrix. The diagonal elements of $\mathbf{S}_\varepsilon$ are set to the noise level estimates, which are calculated from the fit residuals at the pre-processing step. As no spectral correlation between noise levels are assumed, the off-diagonal elements are set to zero. The regularization matrix $\mathbf{R}$ is defined as

$$\mathbf{R}=\mathbf{S}_a^{-1}+\mathbf{T}. \tag{8}$$

Here, $\mathbf{S}_a$ is the a priori covariance matrix and $\mathbf{T}$ the smoothness constraint matrix. For a particular species (in this approach NO_2 and O_3), the elements of the a priori

Discussion Paper | Discussion Paper | Discussion Paper | Discussion Paper |

AMTD

4, 4753–4800, 2011

Validation of SCIAMACHY limb NO_2 profiles

R. Bauer et al.

covariance matrix $\mathbf{S}_a$ are defined for altitudes z_i and z_j as

$$\{\mathbf{S}_a\}_{i,j} = \sigma_i \sigma_j \exp\left(-\frac{|z_i - z_j|}{l_c}\right), \tag{9}$$

where l_c is the correlation length (set to 1.5 km in this approach). σ_i and σ_j are the a priori uncertainties at the altitudes z_i and z_j, respectively. The a priori uncertainties are set to 100 % for NO_2 and 1000 % for O_3, which represents almost non-existent regularization of O_3 from a priori uncertainty. With the smoothness constraint matrix **T** (Rozanov et al., 2011), Tikhonov smoothing is also applied with the smoothing parameter for NO_2 linearly decreasing with altitude from 10 at 50 km to 1.0 at 10 km, i.e. this represents stronger smoothing at high altitudes, while the constraints are weaker at lower altitudes. The smoothing is done to suppress oscillations in the retrieval results while avoiding overconstraining at the same time.

A widely used method to solve the inverse retrieval problem (see Eq. 7) is the optimal estimation with maximum a posteriori information method as described by Rodgers (2000). In this study, however, the information operator approach (Kozlov, 1983; Hoogen et al., 1999; Doicu et al., 2007) is applied instead. The idea and advantage of the information operator approach with respect to the optimal estimation method is that, in the ideal case, only those parameters are used in the fit process, which are determined by the measured information. In this approach, the solution is projected into the space of eigenvectors of the information operator, which is defined by

$$\mathbf{P} = \mathbf{R}^{-1}\mathbf{K}^T\mathbf{S}_\varepsilon^{-1}\mathbf{K}. \tag{10}$$

With the measurement, only an effective state subspace can be accessed, which is limited by considering only eigenvectors whose eigenvalues are larger than a selected threshold value. Employing the Gauss-Newton iterative approach to account for the non-linearity of the inverse problem, the solution at the $(i+1)$-th iterative step is written as

$$\mathbf{x}_{i+1} = \mathbf{x}_i + \sum_{k=1}^{N_i} \beta_{i,k} \boldsymbol{\psi}_{i,k}, \tag{11}$$

where $\boldsymbol{\psi}_{i,k}$ are the eigenvectors of the information operator, **P**. The number of eigenvectors whose eigenvalues are larger than the selected threshold is represented by N_i and the expansion coefficients $\beta_{i,k}$ are given by

$$\beta_{i,k} = \frac{\eta_{i,k}}{c_{i,k}(1+\eta_{i,k})} \boldsymbol{\psi}^T_{i,k} \mathbf{K}_i^T \mathbf{S}_\varepsilon^{-1} \left(\mathbf{y} - \mathbf{y}_i + \mathbf{K}_i (\mathbf{x}_i - \mathbf{x}_0) \right). \tag{12}$$

Here, $\eta_{i,k}$ denotes the eigenvalue of the information operator, **P**, corresponding to the eigenvector $\boldsymbol{\psi}_{i,k}$ and $c_{i,k}$ is the following scalar product:

$$c_{i,k} = \left\langle \mathbf{K}_i^T \mathbf{S}_\varepsilon^{-1} \mathbf{K}_i \boldsymbol{\psi}_{i,k} | \boldsymbol{\psi}_{i,k} \right\rangle. \tag{13}$$

The iterative process is stopped when the maximum difference between the components of the solution vector at two subsequent iterative steps does not exceed 1 %. Typically, three to five iterations are required to achieve the convergence.

The application of the information operator approach to the retrieval of NO_2 vertical profiles from SCIAMACHY limb measurements was previously discussed by Doicu et al. (2007).

2.2 Sensitivity of SCIATRAN NO_2 limb retrieval

The performance of the current retrieval approach is estimated by using two example retrievals. As the atmospheric properties are expected to be different at high latitudes compared with the tropics, one example measurement is at about 77.5° N (see Fig. 1) and the other only slightly north from the equator at 1.5° N, see Fig. 2. Both latitudes

Discussion Paper | Discussion Paper | Discussion Paper | Discussion Paper |

AMTD

4, 4753–4800, 2011

Validation of SCIAMACHY limb NO_2 profiles

R. Bauer et al.

are taken from the average geolocation and ground pixel coordinates of the limb measurement.

It should be noted that in the tropics, the retrieved NO_2 maximum is found at an altitude of about 33 km with 1.4×10^9 molec cm^{-3}, and at high latitudes, it is about 3.0×10^9 molec cm^{-3} at about 20 km altitude.

To illuminate the analysis as displayed in the figures mentioned previously, each feature is explained in detail. The theoretical precisions describe the total retrieval error (noise + smoothing errors) and are calculated from the square root of the diagonal elements of the solution covariance matrix $\hat{\mathbf{S}}$, see Rodgers (2000). $\hat{\mathbf{S}}$ corresponds to the result of the last iteration in the retrieval process $\hat{\boldsymbol{x}}$ and is defined as

$$\hat{\mathbf{S}} = \left(\hat{\mathbf{K}}^T \mathbf{S}_\varepsilon^{-1} \hat{\mathbf{K}} + \mathbf{R}\right)^{-1}. \tag{14}$$

For the tropics, the precisions are worse at lower altitudes than at high latitudes and show similar values as above.

The measurement response given in the same panels is calculated by summing up the area below the averaging kernels. It describes the degree of which the measurements contribute to the retrieved profile. Values close to 1 indicate that the retrieved profiles are mostly unbiased by a priori information.

Comparing the two examples, the response function is generally close to 1 and starts to decrease below 20 km in the tropics and 15 km in the high latitudes, i.e. the lowest altitude unbiased by a priori is lower for the high latitudes. In the tropics, NO_2 values are low with less than 2.0×10^8 molec cm^{-3} below 20 km altitude in the retrieved profile. The influence by the a priori profile with a measurement response greater than 0.9 below 20 km and close to 1 above is small. The NO_2 values in the high latitudes are above 1.0×10^9 molec cm^{-3} between 12 and 15 km, with the lowest measurement response shown here at 12 km. In this case, the measurement response is lower when compared with tropics at this altitude, because the averaging kernels are cut off at 12 km and they contribute more in the high latitudes case.

AMTD
4, 4753–4800, 2011

The averaging kernels are presented in panel (c). As they are calculated on a 1 km grid compared to the resolution of about 3.3 km of the instrument, highest expected values are between 0.3 and 0.4. At about 43 km, averaging kernels are expected to be negative as this is the reference tangent height used for retrieval. This is best seen in Fig. 2. The vertical resolution of the retrieval can be estimated from the width of the averaging kernels which, however, is difficult to quantify. The Backus and Gilbert approach (Backus and Gilbert, 1970, used e.g. in Haley et al., 2004) helps with the definition of a characteristic called spread, calculated with:

$$s(z) = 12\frac{\int (z-z')^2 \mathbf{A}^2(z,z')dz'}{\left[\int |\mathbf{A}(z,z')|dz'\right]^2} \tag{15}$$

The altitude is given as z and $\mathbf{A}$ denotes the averaging kernel matrix. As expected, the spread profiles show the best vertical resolution near the measurement tangent heights.

In the tropics, the spread shows favorable values between 37 and 25 km with values between 2 and less than 6 km. At high latitudes, this range covers 37 to 15 km. Below this 15 km (25 km in the tropics), the low signals resulting from a combination of small NO_2 values and an increasing optical path along the line-of-sight lead to a reduced vertical resolution.

Although these are arbitrary examples, the NO_2 maximum is seen at higher altitudes closer to the equator. In most cases, the altitude range sensitive to NO_2 matches the respective altitudes ranges covered by the occultation instruments used for validation in a reasonable way.

2.3 Photochemical correction of NO_2 for validation

NO_2 is a photochemically active species and has a pronounced diurnal variation. This causes difficulties for validation efforts, as two measurements performed at different local times cannot be compared easily. For the validation of vertical NO_2 profiles, one of these two profiles has to be photochemically corrected with respect to the other one.

To perform this correction, the photochemical box model developed at the University of California, Irvine (Prather, 1992; McLinden et al., 2000) is used to create look-up tables. For three days in a month (1st, 11th and 21st day), on a latitude grid of 2.5° and for an altitude range from 8 to 56 km (step size 2 km, pressure altitudes), complete diurnal circles of NO_2 are stored.

From the NO_2 profiles at the geolocations and times of both measurements, scaling factors can be calculated. In some cases, no matching SZA can be found in the precalculated data. If this happens, the collocation pair is not used for validation. After applying the collocation criteria described later in Sect. 3.1, less than 10 % collocations are discarded due to this problem. For ACE-FTS, this is seen more often, which can be explained with a different orbit resulting in more situations where this seems to be a problem.

The scaling factors are then applied to NO_2 profiles from the occultation instruments (ACE-FTS, SAGE II or HALOE) and the photochemically corrected NO_2 profiles are compared with the matching SCIAMACHY NO_2 profiles.

As discussed by Bracher et al. (2005), the uncertainty of the photochemical correction is estimated to be about 20 %. In this work, however, a look-up-table is used for photochemical corrections instead of full model runs, which might introduce an additional error source. The difference between using full model runs and the look-up-table from the same model is estimated to be less than 10 % above 20 km and can exceed 50 % below this altitude.

2.4 Error discussion

NO_2 retrieval results are influenced by an array of different error sources, and it is important to quantify these in order to decide whether a difference between SCIAMACHY and different satellites is within expectations or not. Generally, retrieval errors contain the smoothing error, the model parameter error, the forward model error and the

Discussion Paper | Discussion Paper | Discussion Paper | Discussion Paper |

AMTD

4, 4753–4800, 2011

Validation of SCIAMACHY limb NO_2 profiles

R. Bauer et al.

retrieval noise. Of these errors, the smoothing error is of less importance here, as it originates from the finite resolution of the instrument with respect to the true state. We do not know the true state and perform comparisons with measurements from real instruments instead, which are also always subject to smoothing errors depending on their resolution. The NO_2 products discussed here show reasonably similar vertical resolutions in the range of 2 to 4 km (see Sect. 3.2).

For each SCIAMACHY NO_2 limb profile, theoretical precisions are provided, as described in Sect. 2.2. They are below 10 % for altitudes between 25 km and 35 km and below 15 % for altitudes between 22 and 42 km (tropics) or 16 and 42 km (high latitudes).

Errors in the temperature and pressure profiles have an insignificant influence on SCIATRAN $NO2_2$ retrieval results in limb mode (less than 5 %) above 20 km as discussed in Rozanov et al. (2005), as accurate ECMWF data are used in the retrieval process.

The influence of aerosols on NO_2 limb retrieval results for SCIAMACHY is estimated by using synthetic retrievals. The retrieval examples shown in Figs. 1 and 2 are used for a forward simulation perturbed with two volcanic scenarios for the stratosphere from LOWTRAN (Kneizys et al. (2002), aged aerosols from moderate volcanic activity and fresh aerosols from high volcanic activity) and a scenario with no aerosols in the forward model, all seen in Fig. 3. Above 22 to 25 km, the influence of aerosols is small (less or about 5 %) for all investigated scenarios and is considered larger below this altitude. For the tropical scenario, the relative errors at low altitudes should be read with care, as very low NO_2 values overemphasize the relative error. Because of a low volcanic activity during the time period considered in this paper, the typical influence of the stratospheric aerosol on the retrieval results is expected to be low.

Pointing errors (i.e. uncertainties in the tangent point altitudes given for the measurements of SCIAMACHY) are estimated to be below 200 m in SCIAMACHY Level 1 data version 6.03 (von Savigny et al., 2009). It is worth mentioning that version 6.03 introduced improvements in pointing accuracy with respect to previous versions, as

AMTD
4, 4753–4800, 2011

discussed in von Savigny et al. (2007). Simulations were done shifting the measurement tangent heights by ±200. Then, the retrievals were done assuming no pointing shift, see Fig. 4. For the high latitudes, the relative deviation of the perturbed scenario with respect to the scenario without a change in altitude does not exceed 5 %. In the tropics, the relative difference is below 12 % above 22 km and exceeds 50 % at 15 km, as the absolute NO_2 values are very low at these altitudes.

To estimate the influence of cloud contamination on NO_2 profiles, a series of synthetic retrievals is performed for clouds of different altitudes, geometrical thickness, optical thickness τ, different SZA, and for both water and ice clouds. These were simulated in the SCIATRAN forward model. Figure 5 shows the influence of the water clouds with different geometrical and optical thickness on the retrieval results at a SZA of 35°. In this case, the relative difference above 25 km is smaller than 6 %. The results for ice clouds are almost identical for this SZA and, hence, not shown here. A maximum relative difference of about 6 % above 17 km is found for a SZA of 70° for both water (Fig. 6) and ice clouds (Fig. 7). It should be noted that a cloud with a top altitude of 15 km is not very likely to be found at high latitudes. For the investigation at lower altitudes or to avoid clouds of higher altitudes (PSCs, NLCs), the SCIAMACHY NO_2 product includes results from SCODA, as mentioned in Sect. 2.1. We applied this method for cloud masking on the results in this paper for testing purposes. However, while about two thirds of all collocations are sorted out, the results do not show any significant difference or improvement. To keep the collocations and as altitudes below 20 km are already difficult to analyze due to other errors described here, it was decided not to apply cloud masking here.

The diurnal variation of NO_2 also affects the retrieval results directly. This problem is not solved with the photochemical corrections applied here and will be referred to as the diurnal effect error, see McLinden et al. (2006). It is related to the changing SZA along the line of sight for a limb or occultation measurement that is not accounted for in the retrieval. The high gradient of NO_2 during sunrise and sunset introduces significant errors. This error has a similar order of magnitude at high SZAs close to

90° for SCIAMACHY NO_2 as for occultation instruments. In the tropics, this error is expected to be small for SCIAMACHY, since the measurements are taken with smaller SZAs resulting in a less rapid change in NO_2 in the line of sight. When estimating the influence of the diurnal effect on the comparison results in this study, we always assume the effect to be small for SCIAMACHY retrievals, which is strictly true only for not too large SZAs.

Precalculated synthetic retrievals from occultation instruments on a 2.5°-latitude grid with the diurnal effect considered in the forward model $\boldsymbol{x}_{\text{sim.w.}}$ and without the diurnal effect in the forward model $\boldsymbol{x}_{\text{sim.}}$ are used to estimate the diurnal effect error for individual occultation measurements:

$$\boldsymbol{\epsilon}_{\text{diurnal}} = \frac{\boldsymbol{x}_{\text{sim.w.}} - \boldsymbol{x}_{\text{sim.}}}{\boldsymbol{x}_{\text{sim.}}} \tag{16}$$

The results from these calculations are discussed in Sect. 3.3.

3 Validation of NO_2

All NO_2 data products used for validation described in this work are retrieved from solar occultation measurements. While HALOE (Halogen Occultation Experiment) and SAGE II (Stratospheric Aerosol Gas Experiment) ceased operations in 2005, the newer instrument ACE-FTS (Atmospheric Chemistry Experiment-Fourier Transform Spectrometer) continues to deliver measurements as of 2011. If available, number densities are taken directly from the data sets (SAGE II) or converted from volume mixing ratios using the pressure and temperature profiles provided in these data sets (HALOE, ACE-FTS).

3.1 Collocation criteria for validation

Allowed pairs of measurements for validation were chosen to have a maximum spatial difference of 500 km and a maximum time difference of 8 h. In addition, tropopause heights at geolocations of both measurements are required to differ not more than 2 km, unless both are below 10 km. The tropopause heights are calculated from ECMWF pressure and temperature profiles using the method from Hoinka (1998) and provided for a $1.5^{\circ} \times 1.5^{\circ}$ grid (Felix Ebojie, personal communication, 2010), from which the nearest neighbor is selected. To avoid comparisons of profiles at different vortex conditions, the potential vorticity at the isentropic level of 475 K is analyzed in the same way as described by Bracher et al. (2004). The potential vorticities are calculated from the UKMO (United Kingdom Meteorological Office) assimilated meteorological data set (with a grid of $3.75^{\circ} \times 2.5^{\circ}$) with the method described in Sonkaew (2010). The collocations are used for validation if the potential vorticity for both measurements is similar, i.e. either below −40 PVU, or above 40 PVU or in the range from −30 to 30 PVU. These criteria can be applied automatically, which allows numerous comparisons.

3.2 Satellite instruments used for validation

The Stratospheric Aerosol Gas Experiment (SAGE II) instrument (Chu et al., 1989) was on board the Earth Radiation Budget Satellite (ERBS) launched in 1984. As the ERBS had a very long operational time (21 yr), there is a long overlap of several years with SCIAMACHY from 2002 to 2005. With SAGE II, aerosols, ozone, NO_2, and water vapour were measured. For SAGE II NO_2, the vertical resolution is about 2 km (Gordley et al., 1996), the field of view of the instrument is 0.5 km. SAGE II Version 6.2 data products are used in this study.

Errors for SAGE II are less than 10 % to 5 % from data sets for altitudes between 25 km for up to 35 km for most measurements. Below 25 km, errors can reach values of about 50 % at 20 km and exceed 10 % above 35 km. These values include altitude uncertainty, profile temperature errors which affect the removal of the Rayleigh-scattered contributions, errors from the removal of ozone and aerosol contributions, and measurement errors, see Cunnold et al. (1991).

Launched on 12 September 1991, the UARS satellite (Upper Atmosphere Research Satellite) carried several instruments for the investigation of the Earth's atmosphere.

AMTD
4, 4753–4800, 2011

One of its ten instruments is the Halogen Occultation Experiment (HALOE, Russell III et al., 1993; Russel III and Remsberg, 2010). HALOE was intended to perform solar occultation measurements of ozone (O_3), hydrogen chloride (HCl), hydrogen fluoride (HF), methane (CH_4), water vapour (H_2O), NO, NO_2 (Gordley et al., 1996) and aerosol extinction at 4 infrared wavelengths. Additionally, pressure and temperature vertical profiles were also retrieved. The satellite has been deactivated in December 2005.

In this study, HALOE Version 19 data which have been screened for cirrus clouds are used for validation (Hervig and McHugh, 1999). A correction for the diurnal effect is also applied. The vertical resolution of NO_2 data is 2 km. The data include random noise error plus aerosol induced error as uncertainties, as discussed in Gordley et al. (1996), along with an estimated total error not including aerosol related errors. For HALOE, this total error is smaller than 10 % between 25 km and 35 km, smaller than 20 % between 25 and 40 km and is larger than 40 % below 20 km.

One of the instruments of SCISAT-1, a Canadian satellite launched in August 2003, is ACE-FTS (Atmospheric Chemistry Experiment-Fourier Transform Spectrometer, Walker et al., 2005; Bernath et al., 2005). Still operational as of 2011, ACE-FTS allows a validation of more recent results compared to SAGE II and HALOE. Including NO_2 and O_3, the ACE-FTS instrument is able to perform measurements on a large variety of atmospheric species. The vertical resolution of the measurements is 3 to 4 km based on the field of view of ACE-FTS (1.25 mrad).

In this study, ACE-FTS Level 2 version 2.2 data products are used, see Boone et al. (2005) for the retrieval method. The uncertainties given are the statistical fitting errors from the least-squares process with a normal distribution of errors assumed (Kerzenmacher et al., 2008). These errors are given as less than 5 % in the altitude range used for analysis (20 to 40 km), while the errors are higher than 10 % below 20 km and exceed 40 % at 15 km.

However, because of the different calculation methods and included error sources, the uncertainty values are not easily comparable.

AMTD
4, 4753–4800, 2011

3.3 Validation results

The validation results are shown as averaged profiles (for SCIATRAN profiles and the respective photochemically corrected profile) with standard deviations. Also, for each altitude h the relative difference RD is displayed for each case, defined as:

$$\mathrm{RD}(h) = \frac{x_{\mathrm{SCIA}}(h) - x_{\mathrm{Val}}(h)}{(\overline{x_{\mathrm{SCIA}}}(h) + \overline{x_{\mathrm{Val}}}(h)) \times 0.5}, \tag{17}$$

with x_{SCIA} as SCIAMACHY NO_2 number densities and x_{Val} as number densities from the respective validation source. The profiles are normalized with respect to the average of the mean SCIAMACHY NO_2 profile $\overline{x_{\mathrm{SCIA}}}$ and the mean profile from the validation source $\overline{x_{\mathrm{Val}}}$. This definition avoids the problem of overemphasized relative deviations, if one of the profiles selected for normalization is very small.

In Fig. 8, a comparison for the profiles in 2003 is given for SAGE II and SCIAMACHY with 1101 comparisons, after all collocation criteria are applied as mentioned in Sect. 3.1. Of these 1101 cases, 560 SAGE II measurements were performed during sunset and 541 during sunrise. In the upper panel, the black line denotes averaged NO_2 values for SCIAMACHY retrieval results with the standard deviations shown as black dashed lines on both sides of this profile. Averaged photochemically corrected NO_2 profiles from the reference data set (SAGE II in this Figure) are shown as a solid red profile, the corresponding standard deviations can be seen as red dashed lines. The lower panel shows relative differences (see Eq. 17) with a red solid line, and the relative difference with its standard deviation subtracted and added as a dashed red line. A grey vertical solid line marks the relative difference 0 as reference. For altitudes above 20 km, the relative difference is typically less than or about 10 %, which is a good agreement between the two instruments. From the studies in Bracher et al. (2005), SAGE II 6.2 NO_2 profiles are expected to be higher than SCIAMACHY, which agrees with the results here, as SCIAMACHY results are smaller than SAGE II values at altitudes lower than 30 km.

AMTD
4, 4753–4800, 2011

In comparison, for 2004 with 1237 collocated pairs (544 sunset, 693 sunrise SAGE II), the mutual agreement is better than 10 % for all altitudes above 18 km, see Fig. 9. From SAGE II comparisons alone, the overall agreement looks very good in both years. There is also data available for the years 2002 and 2005, but only for the last four months (2002) or the first half of the year (2005). Thus, seasonal differences might dominate in these comparisons.

To investigate regional differences, comparisons from 2003 and 2004 are merged and averaged for three latitude ranges. The regions are the northern high latitudes (90° N to 60° N), mid latitudes (60° N to 30° N) and tropics (30° N to 30° S), see Fig. 10. From these three scenarios, the agreement is best at high latitudes, with less than 10 % mean relative difference between 20 km and 36 km. As mentioned earlier, higher SAGE II NO_2 values conform to previous studies. In mid latitudes, relative differences are higher and an agreement better than 10 % is only achieved at altitudes above 23 km. In absolute values, the agreement is better since the NO_2 profiles in this latitude region are smaller compared to Northern latitudes on average. For tropical values, the averaged photochemically corrected SAGE II results are lower than averaged SCIAMACHY values, and the agreement is only better than 10 % above 25 km. This can partly be explained by the low NO_2 values in the tropics scenario, which results in overemphasized relative differences, especially at lower altitudes. Also, the uncertainty of the photochemical correction increases from high latitudes to tropics.

An important error source is the diurnal effect error. NO_2 concentrations are always underestimated if the diurnal effect is not considered. Since it is known to vary depending on latitude and season (Brohede et al., 2007), an individual error estimation is calculated for each collocation pair. In Fig. 11 panel (a), mean values for the relative diurnal effect error are calculated for the latitudinal zones and profiles in Fig. 10. The error is calculated using Eq. (16). The diurnal effect error is lower for the high latitude case, where the agreement is also considered best.

To estimate the influence that this error has on retrieved NO_2 profiles, it is added to the averaged photochemically corrected SAGE II NO_2 profiles in panels (b) and (d) of Fig. 11. Each photochemically corrected profile is compensated with the matching estimated diurnal effect error. This is not done for high latitudes, as the SCIAMACHY profiles with high SZA are also expected to be influenced by the diurnal effect error in a similar order of magnitude. Although the agreement is improved for the mid latitudes for altitudes below 25 km, it worsens for the tropics in this case for all altitudes. Panels (c) and (e) show the relative differences after scaling with the relative diurnal effect error.

Similar to SAGE II, available data allow a comparison of the years 2003 and 2004 for HALOE. For 2003, a total of 895 comparisons are performed, of which 285 are done during HALOE sunset and 610 during sunrise. The relative differences (see Fig. 12) are similar in magnitude compared to SAGE II, with a difference of up to 10 % for altitudes higher than 20 km and rises up to 45 % for altitudes of 15 km. In absolute numbers (number densities, see upper panel), the averaged and photochemically corrected HALOE profiles are higher than for SCIAMACHY around the profile maximum (∼28 km) and lower below 20 km. For 2004 (see Fig. 13), a high number of 1632 comparisons (618 at HALOE sunset and 1014 at sunrise) is investigated with similar numbers as for 2003. The difference at altitudes below 22 km is higher and exceeds 50 %. Above this altitude, the agreement is still better than 10 %.

Different latitude regions are investigated in Fig. 14 with the same approach as for SAGE II. Comparisons from the years 2003 and 2004 are used and three latitude regions are investigated, i.e. the high latitudes (60° N to 90° N), middle latitudes (30° N to 60° N) and tropics (30° S to 30° N). For high latitudes, the agreement is better than 10 % for altitudes above 21 km with a larger difference below this altitude. The collocation pairs feature lower absolute values in the other two regions and larger differences as compared to high latitudes. Although the difference between the averaged profiles in absolute numbers is not larger than that for high latitudes, lower NO_2 values at low altitudes inflate the values for relative comparisons. Contrary to SAGE II, it is the SCIAMACHY retrieval that features higher NO_2 for HALOE, at least for altitudes below 20 km. Because HALOE NO_2 retrieval applies a correction for the diurnal effect error,

AMTD
4, 4753–4800, 2011

it is not discussed here.

The third instrument to be investigated is ACE-FTS. Because of the mission time, the years 2004 and 2005 are chosen for investigation. Validation results for 2004 are seen in Fig. 15. The agreement for ACE-FTS is better than 10 % for an altitude range of about 25 to 40 km. A large number of profiles in 2004 (525 collocations, 304 at ACE-FTS sunset, 221 at sunrise) is used for this comparison, and even more (1143 collocations, 513 at sunset, 630 at sunrise) for the year 2005 (see Fig. 16). The averaged NO_2 profile from photochemically corrected ACE-FTS data features a maximum that is slightly lower in altitude compared to the averaged SCIAMACHY NO_2 retrievals, and similar values (up to 10 % lower) above this maximum but higher NO_2 values (up to 40 %) than SCIAMACHY below this maximum. In Kerzenmacher et al. (2008), ACE-FTS NO_2 has been validated with a set of different instruments including SCIAMACHY sun occultation retrieval results, with an agreement better than 20 % (VMR values, wide range of different instruments including HALOE, SAGE II, SAGE III and SCIAMACHY sun occultation measurements, and using a similar chemical box model for photochemical correction).

As above, three latitude regions are selected, the same as for SAGE II and HALOE, see Fig. 17. We averaged collocations from 2004 and 2005. Unfortunately, after applying collocation criteria, the number of usable profile pairs outside the high latitudes is noticeably small. The reason for this is that ACE-FTS performs 50 % of its measurements in the polar regions (south of 60° S and north of 60° N), resulting in a lower number of collocations in the tropics. While the agreement is worse in the tropics compared to the two other regions, only 117 profiles from two years are available for averaging. Similar to SAGE II, the diurnal effect error is investigated, see Fig. 18, panel (a).

With the same method used for SAGE II, the possible influence from the diurnal effect for middle latitudes (panel b) and tropics (panel e) is investigated by adding the estimated diurnal effect error to averaged ACE-FTS profiles from Fig. 17. Although the agreement becomes worse above 25 km, it is considerably improved below this altitude for both tropics and middle latitudes.

Summing up the results from the three instruments, the agreement is considered best at high latitudes and all three instruments show a comparable agreement with SCIAMACHY, although distinct features are seen. Higher NO_2 values at lower altitudes are one of the reasons for the better agreement at the high latitude cases. Additionally, the SCIAMACHY measurements at high latitudes feature higher SZAs (about 70° to slightly below 90°) compared to measurements in the tropics, where an SZA of 30° is common. Thus, for the high latitudes, smaller photochemical corrections are required depending on altitude. NO_2 concentrations change rapidly at daybreak and change a lot less during the day at most investigated altitudes here. Still, the photochemical correction method can not be excluded as a significant error source. Due to this, the altitude range of the three occultation instruments varies and the number of averaged profiles is also smaller at low altitudes. For example, 572 HALOE profiles are averaged at most altitudes in the tropics. This number goes down to 563 at 18 km and decreases further to only 492 valid profiles at 15 km. However, these numbers are still reasonably high. It is worth mentioning that the profiles were not smoothed, i.e. differences in resolution have not been accounted for. Also, estimating the change of including the diurnal effect error in photochemically corrected profiles results in improvements in 3 of 4 cases for SAGE II and ACE-FTS for altitudes below 25 km, where the diurnal effect error shows the highest values.

For these three validation sets, the mean relative deviation (MRD) is calculated in the altitude region 20 to 40 km, see Table 1. MRD values where diurnal scaling has been applied were available. Because this only improves the agreement below 25 km (with one exception), these MRD values for 20 to 40 km are not smaller than without diurnal scaling. 727 to 1767 collocations are taken into account for each year and instrument for the whole globe and for all seasons. The MRD values can be very different from year to year in this data set for the same instrument. In this comparison, SAGE II NO_2 is high compared to that of SCIAMACHY in 2003 (2 % to −14 %, on average −4 %), but lower in 2004 (8 % to −9 %, on average 1 %). In Bracher et al. (2005), SAGE II NO_2 values were found to be high in comparison to SCIAMACHY with

MRD of −10 % to −35 % between 20 and 38 km. However, these values apply only to a subset of measurements with an SZA range of 60 to 70°, only sunset measurements and only for the year 2003. If we limit the collocations for the SAGE II comparisons by applying similar restrictions, i.e. only altitudes of 20 to 40 km, the same SZA range and no sunrise measurements, the MRD values lie between −7 % and −30 %, on average −17 %. If the MRD are normalized in the same way as in Bracher et al. (2005), the MRD values lie between −8 % and −39 %, which agree very well with the known results.

4 Conclusions

This work gives an overview of the performance and sensitivity of SCIAMACHY NO_2 limb retrieval focusing mainly on a range of occultation instruments (SAGE II, HALOE, ACE-FTS).To address the problem of high diurnal variability of NO_2, photochemical corrections are applied. The diurnal effect error that originates from changing SZA along the line of sight for individual measurements is also discussed. The results are summarized in Table 1.

For this work, thousands of profile pairs are investigated after applying collocation criteria, using data from two years and over the whole globe for each instrument. As regards the three occultation instruments used for validation, SAGE II has a mean relative difference of less than 10 % with SCIAMACHY for altitudes above 22 km in both years (2003 and 2004). For HALOE, the agreement is likewise good (mean rel. difference less than 10 % between 22 and 40 km for both years), with higher differences at low altitudes. For ACE-FTS, the mean relative difference is less than 10 % above 24 km in 2004, above 23 km in 2005, and below 40 km (for both years).

Due to the different operation times of the instruments, the years 2004 and 2005 are investigated for ACE-FTS, while SAGE II and HALOE analysis is done for 2003 and 2004. Altitudes below 20 km are seen with higher differences than 10 % for all instruments. However, the error discussion shows that uncertainties from different sources including aerosols and clouds can have a significant impact below this altitude.

AMTD
4, 4753–4800, 2011

Retrieval and validation of NO_2 in limb mode at 15 km and below is a challenge that is beyond the scope of this work, but is expected to provide interesting insights in the composition and sources of atmospheric pollution.

The data basis allowed us a closer look at different latitudinal regions. For high latitudes (90° N to 60° N) and middle latitudes (60° N to 30° N), the agreement is better than in the tropics (30° N to 30° S) for all instruments used for validation. Possible reasons for this are most likely the diurnal effect error, low NO_2 values, and small SZAs for SCIAMACHY, among others, which may result in a less accurate photochemical correction.

To conclude, this work is expected to contribute to investigations of NO_2 amounts and emissions for which validated long-term data sets are of great importance.

Acknowledgements. We are thankful to ECMWF for providing pressure and temperature information (ECMWF Special Project SPDECDIO) for this study. Some data shown here were calculated on German HLRN (High-Performance Computer Center North). Services and support provided by the Atmospheric ChemistryExperiment (ACE), also known as SCISAT, a Canadian-led mission mainly supported by the Canadian Space Agency and the Natural Sciences and Engineering Research Council of Canada, are greatly appreciated. Our gratitude also goes to the HALOE science and data processing teams for providing the profiles used in this study. We wish to thank the NASA Langley Research Center (NASA-LaRC) and the NASA Langley Radiation and Aerosols Branch for making it possible for us to work with SAGE II data sets. This study has been funded by the University and State of Bremen.

References

Backus, G. and Gilbert, F.: Uniqueness in the inversion of inaccurate gross earth data, Philosophical Transactions of the Royal Society of London. Series A, Mathematical and Physical Sciences, 266, 123–192, 1970. 4763

Bernath, P. F., McElroy, C. T., Abrams, M. C., Boone, C. D., Butler, M., Camy-Peyret, C., Carleer, M., Clerbaux, C., Coheur, P.-F., Colin, R., DeCola, P., DeMazire, M., Drummond, J. R., Dufour, D., Evans, W. F. J., Fast, H., Fussen, D., Gilbert, K., Jennings, D. E., Llewellyn, E.

J., Lowe, R. P., Mahieu, E., McConnell, J. C., McHugh, M., McLeod, S. D., Michaud, R., Midwinter, C., Nassar, R., Nichitiu, F., Nowlan, C., Rinsland, C. P., Rochon, Y. J., Rowlands, N., Semeniuk, K., Simon, P., Skelton, R., Sloan, J. J., Soucy, M.-A., Strong, K., Tremblay, P., Turnbull, D., Walker, K. A., Walkty, I., Wardle, D. A., Wehrle, V., Zander, R., and Zou, J.: Atmospheric chemistry experiment (ACE): mission overview, Geophys. Res. Lett., 32, L15S01, doi:10.1029/2005GL022386, 2005. 4755, 4769

Bogumil, K., Orphal, J., Voigt, S., Bovensmann, H., Fleischmann, O. C., Hartmann, M., Homann, T., Spietz, P., Vogel, A., and Burrows, J. P.: Reference spectra of atmospheric trace gases measured with the SCIAMACHY PFM satellite spectrometer, in: Proc. 1st Europ. Sympos. Atmos. Meas. from Space (ESAMS-99), 2, 443–447, ESA-ESTEC, Noordwijk, 1999. 4757

Boone, C., Nassar, R., Walker, K., Rochon, Y., McLeod, S., Rinsland, C., and Bernath, P.: Retrievals for the atmospheric chemistry experiment Fourier-transform spectrometer, Appl. Optics, 44, 7218–7231, 2005. 4769

Bovensmann, H., Burrows, J. P., Buchwitz, M., Frerick, J., Noël, S., Rozanov, V., Chance, K., and Goede, A.: SCIAMACHY: Mission objectives and measurement modes, J. Atmos. Sci., 56, 127–150, 1999. 4755, 4756

Bracher, A., Weber, M., Bramstedt, K., Tellmann, S., and Burrows, J. P.: Long-term global measurements of ozone profiles by GOME validated with SAGE II considering atmospheric dynamics, J. Geophys. Res., 109, D20308, doi:10.1029/2004JD004677, 2004. 4768

Bracher, A., Sinnhuber, M., Rozanov, A., and Burrows, J. P.: Using a photochemical model for the validation of NO_2 satellite measurements at different solar zenith angles, Atmos. Chem. Phys., 5, 393–408, doi:10.5194/acp-5-393-2005, 2005. 4764, 4770, 4774, 4775

Brohede, S., Haley, C., McLinden, C., Sioris, C., Murtagh, D., Petelina, S. V., Llewellyn, E. J., Bazureau, A., Goutail, F., Randall, C., Lumpe, J. D., Taha, G., Thomasson, L. W., and Gordley, L. L.: Validation of Odin/OSIRIS stratospheric NO_2 profiles, J. Geophys. Res., 112, D07310, doi:10.1029/2006JD007586, 2007. 4771

Burrows, J. P., Hötzle, E., E., Goede, A., Visser, H., and Fricke, W.: SCIAMACHY – scanning imaging absorption spectrometer for atmospheric chartography, Acta Astronautica, 35, 445–451, 1995. 4755, 4756

Chu, W. P., McCormick, M. P., Lenoble, J., Brogniez, C., and Pruvost, P.: SAGE II inversion algorithm, J. Geophys. Res., 94, 8339–8351, 1989. 4755, 4768

Crutzen, P.: The influence of nitrogen oxides on the atmospheric ozone content, Q. J. Roy.

Meteor. Soc., 96, 320–325, 1970. 4754
Cunnold, D. M., Zawodny, J. M., Chu, W. P., Pommereau, J. P., Goutail, F., Lenoble, J., McCormick, M. P., Veiga, R. E., Murcray, D., Iwagami, N., et al.: Validation of SAGE II NO_2 Measurements, J. Geophys. Res., 96, 12913–12925, 1991. 4768
Doicu, A., Hilgers, S., von Bargen, A., Rozanov, A., Eichmann, K.-U., von Savigny, C., and Burrows, J. P.: Information Operator Approach and iterative regularization methods for atmospheric remote sensing, J. Quant. Spectrosc. Ra., 103, 340–350, 2007. 4760, 4761
Eichmann, K.-U., von Savigny, C., Reichl, P., Robert, C., Steinwagner, J., Bovensmann, H., and Burrows, J. P.: SCODA: SCIAMACHY Cloud Detection Algorithm from Limb Radiance Measurements – ALGORITHM THEORETICAL BASIS DOCUMENT, Tech. rep., Institute of Environmental Physics, University of Bremen, unpublished technical document, 2009. 4758
Gordley, L. L., Russell III, J. M., Mickley, L. J., Frederick, J. E., Park, J. H., Stone, K. A., Beaver, G. M., McInemey, J. M., Deaver, L. E., Toon, G. C., et al.: Validation of nitric oxide and nitrogen dioxide measurements made by the Halogen Occultation Experiment for UARS platform, J. Geophys. Res.-Atmos., 101, 10241–10266, 1996. 4768, 4769
Haley, C. S., Brohede, S. M., Sioris, C. E., Griffioen, E., Murtagh, D. P., McDade, I. C., Eriksson, P., Llewellyn, E. J., Bazureau, A., and Goutail, F.: Retrieval of stratospheric O_3 and NO_2 profiles from Odin Optical Spectrograph and Infrared Imager System (OSIRIS) limb-scattered sunlight measurements, J. Geophys. Res., 109, D16303, doi:10.1029/2004JD004588, 2004. 4759, 4763
Hervig, M. and McHugh, M.: Cirrus detection using HALOE measurements, Geophys. Res. Lett., 26, 719–722, 1999. 4769
Hoinka, K.: Statistics of the global tropopause pressure, Mon. Weather Rew., 126, 3303–3325, 1998. 4768
Hoogen, R., Rozanov, V. V., and Burrows, J. P.: Ozone profiles from GOME satellite data: Algorithm description and first validation, J. Geophys. Res., 104, 8263–8280, doi:10.1029/1998JD100093, 1999. 4760
Kerzenmacher, T., Wolff, M. A., Strong, K., Dupuy, E., Walker, K. A., Amekudzi, L. K., Batchelor, R. L., Bernath, P. F., Berthet, G., Blumenstock, T., Boone, C. D., Bramstedt, K., Brogniez, C., Brohede, S., Burrows, J. P., Catoire, V., Dodion, J., Drummond, J. R., Dufour, D. G., Funke, B., Fussen, D., Goutail, F., Griffith, D. W. T., Haley, C. S., Hendrick, F., Höpfner, M., Huret, N., Jones, N., Kar, J., Kramer, I., Llewellyn, E. J., López-Puertas, M., Manney, G., McElroy, C. T., McLinden, C. A., Melo, S., Mikuteit, S., Murtagh, D., Nichitiu, F., Notholt, J., Nowlan, C.,

AMTD
4, 4753–4800, 2011

Validation of SCIAMACHY limb NO_2 profiles

R. Bauer et al.

Piccolo, C., Pommereau, J.-P., Randall, C., Raspollini, P., Ridolfi, M., Richter, A., Schneider, M., Schrems, O., Silicani, M., Stiller, G. P., Taylor, J., Tétard, C., Toohey, M., Vanhellemont, F., Warneke, T., Zawodny, J. M., and Zou, J.: Validation of NO_2 and NO from the Atmospheric Chemistry Experiment (ACE), Atmos. Chem. Phys., 8, 5801–5841, doi:10.5194/acp-8-5801-2008, 2008. 4769, 4773

Kneizys, F. X., Shettle, E. P., Abreu, L. W., Chetwynd, J. H., and Anderson, G. P.: Users Guide to LOWTRAN 7, Tech. rep., Defense Technical Information Center OAI-PMH Repository [http://stinet.dtic.mil/oai/oai] (United States), http://handle.dtic.mil/100.2/ADA206773, 2002. 4757, 4765

Kozlov, V.: Design of experiments related to the inverse of mathematical physics, in: Mathematical Theory of Experiment Design, edited by: Ermakov, C. M., 216–246, Nauka, Moscow, 1983 (in Russian). 4760

McLinden, C., Olsen, S. C., Hannegan, B., Wild, O., Prather, M. J., and Sundet, J.: Stratospheric ozone in 3-D models: A simple chemistry and the cross-tropopause flux, J. Geophys. Res., 105, 14653, doi:10.1029/2000JD900124, 2000. 4764

McLinden, C., Haley, C., and Sioris, C.: Diurnal effects in limb scatter observations, J. Geophys. Res., 111, D14302, doi:10.1029/2005JD006628, 2006. 4766

Montzka, S. A., Reimann (Coordinatinh Lead Authors), S., Engel, A., Krüger, K., O'Doherty, S., Sturges, W. T., Blake, D., Dorf, M., Fraser, P., Froidevaux, L., Jucks, K., Kreher, K., Kurylo, M. J., Mellouski, A., Miller, J., Nielsen, O.-J., Orkin, V. L., Prinn, R. G., Rhew, R., Santee, M. L., Stohl, A., and Verdonik, D.: Ozone-Depleting Substances (ODSs) and Related Chemicals, in: Scientific Assessment of Ozone Depletion: 2010, Global Ozone Research and Monitoring Project-Report No. 52, chap. 1, 79–80, World Meteorological Organization, Geneva, Switzerland, 2011. 4755

Noël, S., Bovensmann, H., Burrows, J., Frerick, J., Chance, K., Goede, A., and Muller, C.: SCIAMACHY instrument on ENVISAT-1, in: Proceedings of SPIE, vol. 3498, p. 94, 1998. 4757

Platt, U.: Differential optical absorption spectroscopy (DOAS), in: Air Monitoring by Spectroscopic Techniques, edited by: Sigrist, M., 27–84, John Wiley, Hoboken, NJ, 1994. 4758

Portmann, R. W., Brown, S. S., Gierczak, T., Talukdar, R. K., Burkholder, J. B., and Ravishankara, A. R.: Role of nitrogen oxides in the stratosphere: A reevaluation based on laboratory studies, Geophys. Res. Lett., 26, 2387–2390, 1999. 4754

Prather, M.: Catastrophic loss of stratospheric ozone in dense volcanic clouds, J. Geophys.

Res., 97, 10187, doi:10.1029/92JD00845, 1992. 4764
Ravishankara, A. R., Daniel, J. S., and Portmann, R. W.: Nitrous oxide (N_2O): The dominant ozone-depleting substance emitted in the 21st century, Science, 326, 123–125, 2009. 4755
Rodgers, C. D.: Inverse Methods for Atmospheric Sounding, vol. 2 of Series on Atmospheric, Oceanic and Planetary Physics, World Scientific, 2000. 4760, 4762
Rozanov, A.: Sciatran – Radiative transfer model and retrieval algorithm, http://www.iup.uni-bremen.de/sciatran/, 2011. 4757
Rozanov, A., Bovensmann, H., Bracher, A., Hrechanyy, S., Rozanov, V., Sinnhuber, M., Stroh, F., and Burrows, J.: NO_2 and BrO vertical profile retrieval from SCIAMACHY limb measurements: Sensitivity studies, Adv. Space Res., 36, 846–854, 2005. 4765
Rozanov, A., Kühl, S., Doicu, A., McLinden, C., Puķīte, J., Bovensmann, H., Burrows, J. P., Deutschmann, T., Dorf, M., Goutail, F., Grunow, K., Hendrick, F., von Hobe, M., Hrechanyy, S., Lichtenberg, G., Pfeilsticker, K., Pommereau, J. P., Van Roozendael, M., Stroh, F., and Wagner, T.: BrO vertical distributions from SCIAMACHY limb measurements: comparison of algorithms and retrieval results, Atmos. Meas. Tech., 4, 1319–1359, doi:10.5194/amt-4-1319-2011, 2011. 4760
Russel III, J. M. and Remsberg, E. E.: The HALogen Occultation Experiment (HALOE), http://haloe.gats-inc.com, 2010. 4769
Russell III, J. M., Gordley, L. L., Park, J. H., Drayson, S. R., Hesketh, W. D., Cicerone, R. J., Tuck, A. F., Frederick, J. E., Harries, J. E., and Crutzen, P. J.: The halogen occultation experiment, J. Geophys. Res.-Atmos., 98, 10777–10797, 1993. 4755, 4769
Sioris, C. E., Haley, C. S., McLinden, C. A., von Savigny, C., McDade, I. C., McConnell, J. C., Evans, W. F. J., Lloyd, N. D., Llewellyn, E. J., Chance, K. V., Kurosu, T. P., Murtagh, D., Frisk, U., Pfeilsticker, K., Bosch, H., Weidner, F., Strong, K., Stegman, J., and Megie, G.: Stratospheric profiles of nitrogen dioxide observed by Optical Spectrograph and Infrared Imager System on the Odin satellite, J. Geophys. Res., 108, 4215, doi:10.1029/2002JD002672, 2003. 4759
Sonkaew, T.: Quantification of the chemical ozone loss in the northern and southern polar vortices using SCIAMACHY limb measurements, Ph.D. thesis, University of Bremen, 2010. 4768
von Savigny, C., Ulasi, E. P., Eichmann, K.-U., Bovensmann, H., and Burrows, J. P.: Detection and mapping of polar stratospheric clouds using limb scattering observations, Atmos. Chem. Phys., 5, 3071–3079, doi:10.5194/acp-5-3071-2005, 2005. 4758

von Savigny, C., Rozanov, A., Bovensmann, H., Noel, S., Gottwald, M., Slijkhuis, S., and Burrows, J.: Studying Envisat attitude with SCIAMACHY limb-scatter measurements, in: Proceedings of the Envisat Symposium, 2007. 4766

von Savigny, C., Bovensmann, H., Bramstedt, K., Dikty, S., Ebojie, F., Jones, A., Noël, S., Rozanov, A., and Sinnhuber, B.-M.: Indications for long-term trends and seasonal variations in the SCIAMACHY Level 1 version 6.03 tangent height information, Tech. rep., Institute of Environmental Physics, University of Bremen, technical note TN-IUP-scia-pointing-2009-01 Issue 2, 2009. 4765

Walker, K. A., Randall, C. E., Trepte, C. R., Boone, C. D., and Bernath, P. F.: Initial validation comparisons for the Atmospheric Chemistry Experiment (ACE-FTS), Geophys. Res. Lett., 32, L16S04, doi:10.1029/2005GL022388, 2005. 4755, 4769

AMTD

4, 4753–4800, 2011

Validation of SCIAMACHY limb NO_2 profiles

R. Bauer et al.

Table 1. Mean relative deviations (MRD) for all comparisons and an altitude range from 20 to 40 km. MRD values with diurnal scaling are given for available latitude bins.

instrument	year	latitudes	SZA	N	MRD (20 km to 40 km)	MRD w. diurn. scal.
SAGE II	2003	all	22.7–89.7	560(SS) & 541(SR)	−4 % (2 % to −14 %)	
	2004	all	23.2–87.2	544(SS) & 693(SR)	1 % (8 % to −9 %)	
	03 & 04	90° N to 60° N	39.1–87.3	581	−10 % (−3 % to −37 %)	
	03 & 04	60° N to 30° N	22.7–76.8	507	−2 % (8 % to −17 %)	2 % (9 % to −17 %)
	03 & 04	30° N to 30° S	22.8–62.3	497	14 % (24 % to 4 %)	22 % (45 % to 11 %)
HALOE	2003	all	22.3–88.8	285(SS) & 610(SR)	2 % (6 % to −7 %)	
	2004	all	22.1–89.7	618 (SS) & 1014 (SR)	2 % (16 % to −5 %)	
	03 & 04	90° N to 60° N	40.4–87.7	574	−4 % (12 % to −20 %)	
	03 & 04	60° N to 30° N	22.1–75.9	549	7 % (33 % to −5 %)	
	03 & 04	30° N to 30° S	22.2–64.4	572	15 % (35 % to 3 %)	
ACE-FTS	2004	all	26.4–89.2	304 (SS) & 221(SR)	−4 % (7 % to −26 %)	
	2005	all	25.1–89.7	513 (SS) & 630 (SR)	−1 % (11 % to −29 %)	
	04 & 05	90° N to 60° N	39.9–89.8	949	−1 % (7 % to −17 %)	
	04 & 05	60° N to 30° N	26.7–85.3	185	5 % (13 % to −11 %)	8 % (16 % to −3 %)
	04 & 05	30° N to 30° S	25.1–56.3	117	−2 % (15 % to −42 %)	5 % (20 % to −25 %)

Discussion Paper | Discussion Paper | Discussion Paper | Discussion Paper |

AMTD

4, 4753–4800, 2011

Validation of SCIAMACHY limb NO_2 profiles

R. Bauer et al.

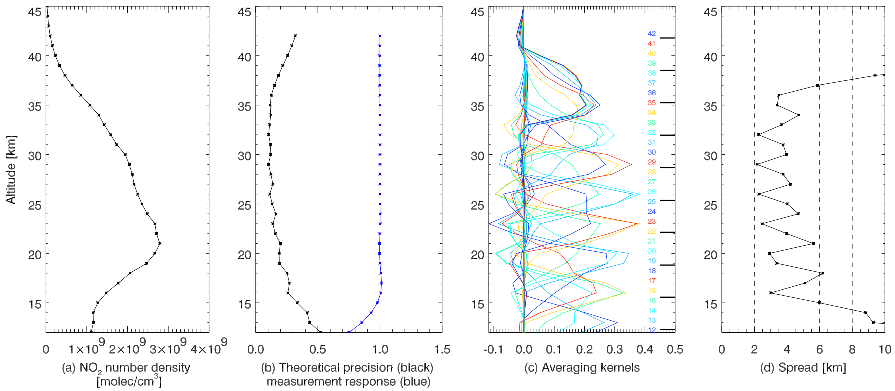

Fig. 1. An example retrieval at about 77.5° N is analyzed to study the sensitivity. The retrieved NO_2 profile is shown in panel **(a)**. Panel **(b)** shows the theoretical precision (black), as well as the measurement response (blue). Panel **(c)** displays the respective averaging kernels, color coded for altitude levels. Panel **(d)** shows the spread of the averaging kernels.

AMTD
4, 4753–4800, 2011

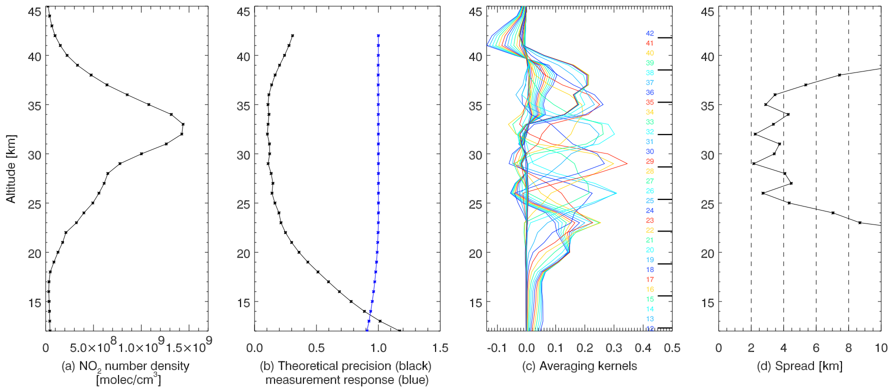

Fig. 2. Similar to Fig. 2, a retrieved NO_2 profile is analyzed. However, this example is obtained at 1.45° N. Panel **(a)** shows the NO_2 profile retrieved with SCIATRAN, panel **(b)** theoretical precision (black) and measurement response (blue), panel **(c)** averaging kernels and panel **(d)** spread.

AMTD
4, 4753–4800, 2011

Validation of SCIAMACHY limb NO_2 profiles

R. Bauer et al.

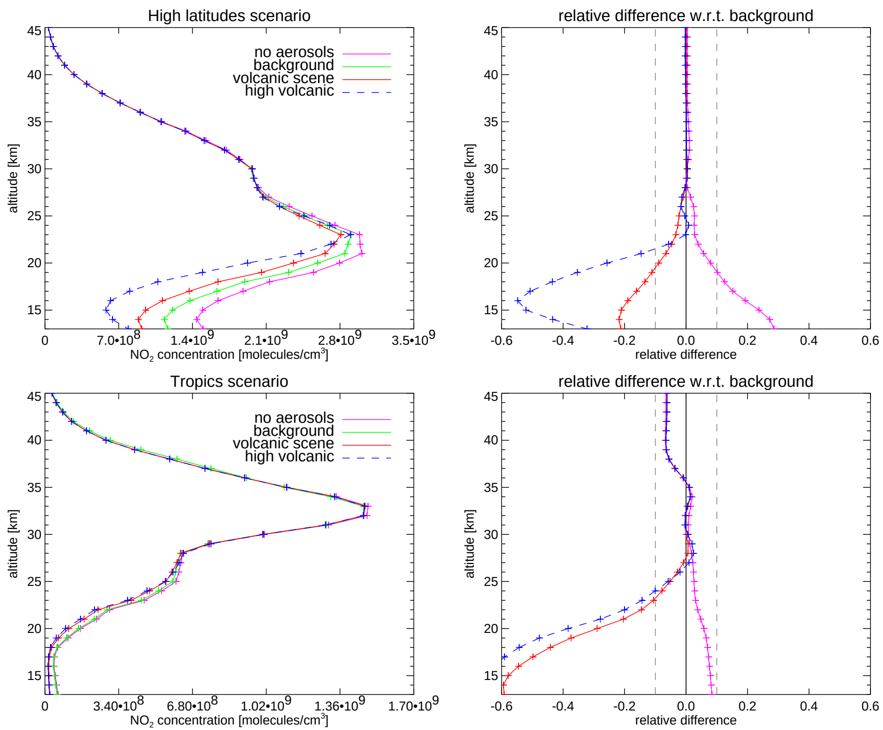

Fig. 3. Influence of the stratospheric aerosols on the retrieved NO_2 profiles. Left panels show NO_2 profiles retrieved for different aerosol loadings at high latitudes (upper panels) and in the tropics (lower panels). Right panels show corresponding relative deviations.

AMTD

4, 4753–4800, 2011

Validation of SCIAMACHY limb NO_2 profiles

R. Bauer et al.

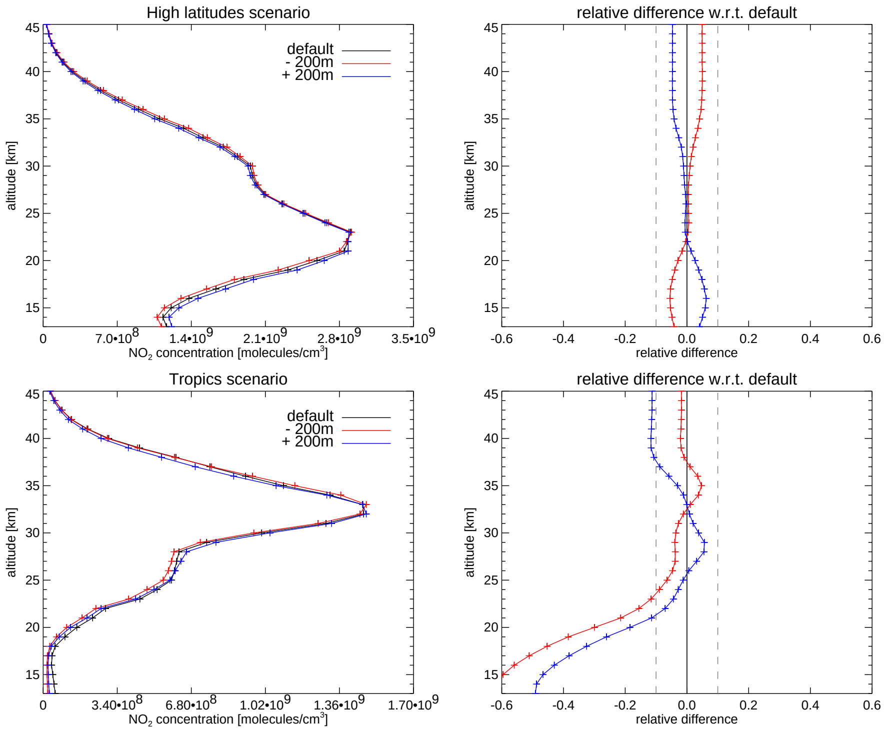

Fig. 4. Influence of the pointing errors on the retrieval results for high latitudes (upper panels) and tropics (lower panels). Left panels show the retrieved profiles for shifted ±200 m and unperturbed tangent heights. Right panels show the corresponding relative deviations.

AMTD

4, 4753–4800, 2011

Validation of SCIAMACHY limb NO_2 profiles

R. Bauer et al.

Title Page
Abstract | Introduction
Conclusions | References
Tables | Figures
◀| |▶
◀ ▶
Back | Close
Full Screen / Esc
Printer-friendly Version
Interactive Discussion

AMTD
4, 4753–4800, 2011

Validation of SCIAMACHY limb NO_2 profiles

R. Bauer et al.

Title Page
Abstract | Introduction
Conclusions | References
Tables | Figures
◂| |▸
◂ ▸
Back | Close
Full Screen / Esc
Printer-friendly Version
Interactive Discussion

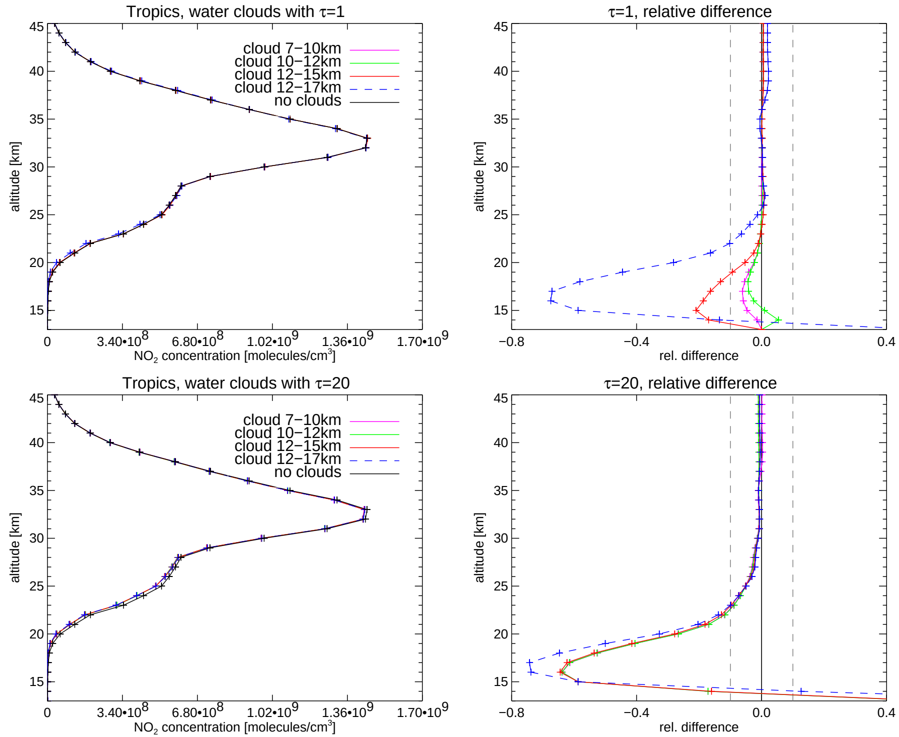

Fig. 5. Influence of water clouds with an optical thickness of 1 (upper panels) and 20 (lower panels) on the retrieved results for the tropics (SZA = 35°). Left panels show the NO_2 profiles retrieved for different clouds. Right panels show corresponding relative deviations.

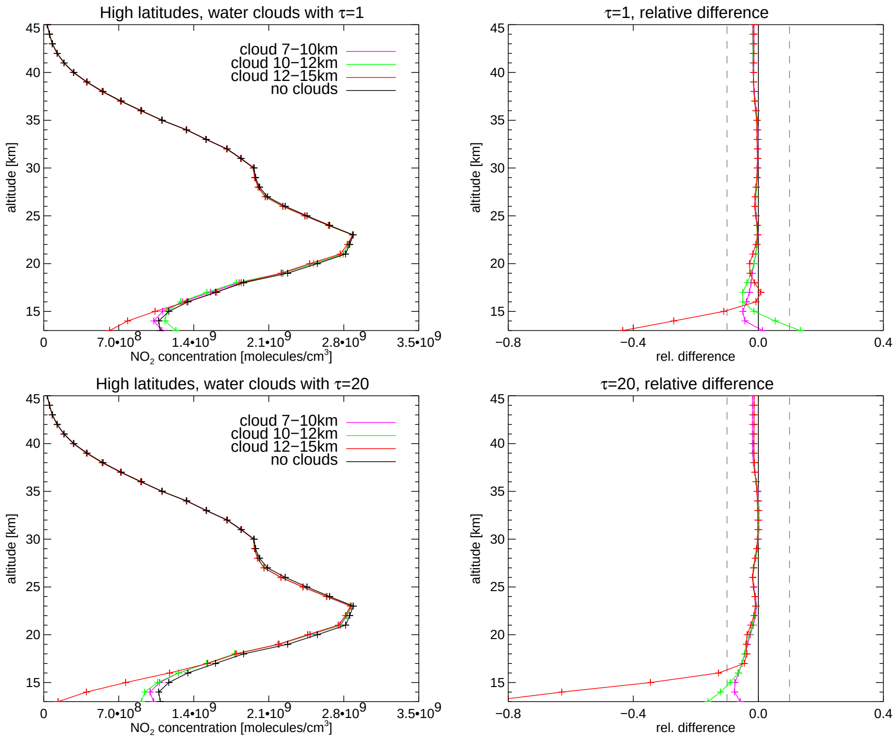

Fig. 6. Same as Fig. 5, but for high latitudes (SZA = 70°), North Hemisphere.

AMTD
4, 4753–4800, 2011

Validation of SCIAMACHY limb NO_2 profiles

R. Bauer et al.

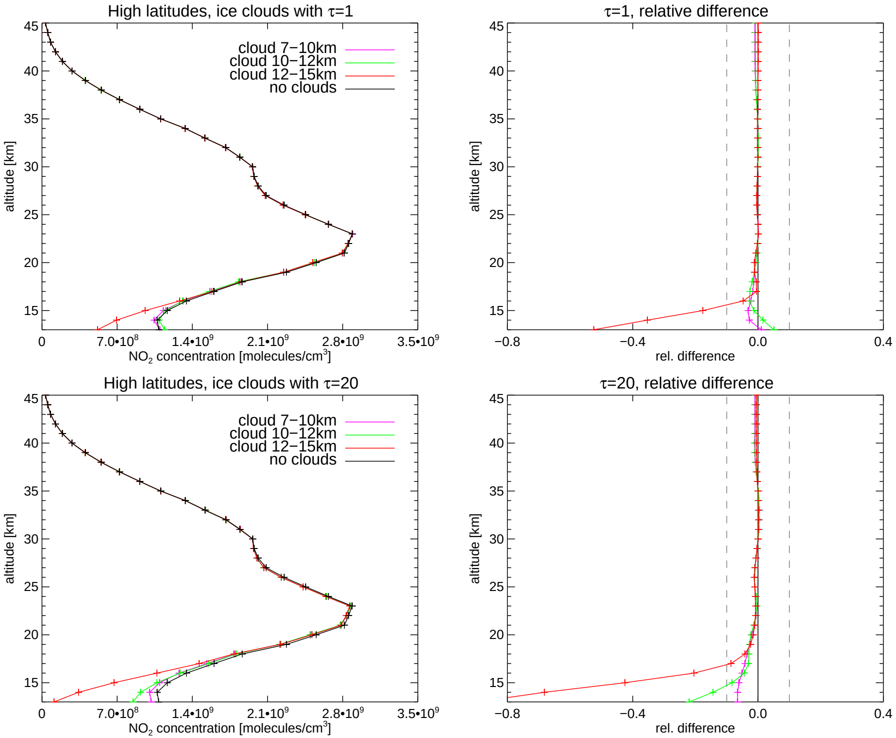

Fig. 7. Same as Fig. 6, but for ice clouds.

AMTD

4, 4753–4800, 2011

Validation of SCIAMACHY limb NO_2 profiles

R. Bauer et al.

Title Page
Abstract | Introduction
Conclusions | References
Tables | Figures
◀| |▶
◀ ▶
Back | Close
Full Screen / Esc
Printer-friendly Version
Interactive Discussion

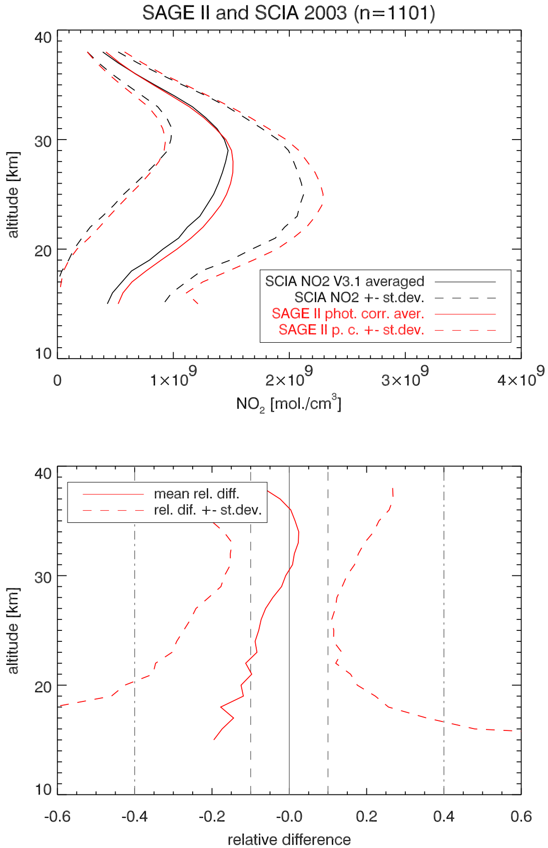

Fig. 8. The upper panel shows averaged photochemically corrected NO_2 profiles from SAGE II and collocated NO_2 profiles retrieved from SCIAMACHY in the year 2003. The lower panel shows relative differences for the same set of profiles.

AMTD
4, 4753–4800, 2011

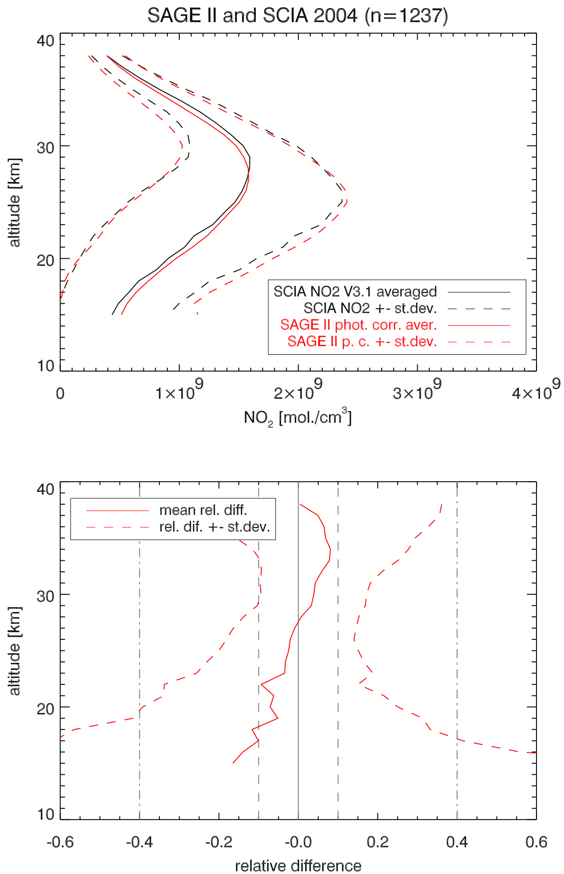

Fig. 9. Same as Fig. 8, but for 2004 data.

AMTD
4, 4753–4800, 2011

Validation of SCIAMACHY limb NO_2 profiles

R. Bauer et al.

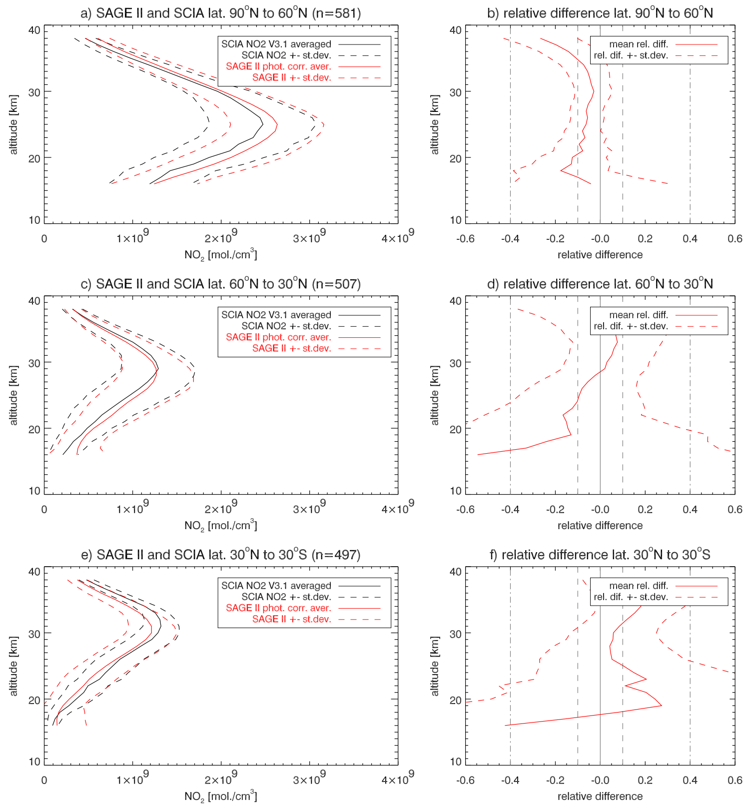

Fig. 10. From the SAGE II collocation pairs for 2003 and 2004, subsets for different latitude ranges are investigated. Panels **(a)** and **(b)** are restricted to northern latitudes (60° N to 90 ° N), panels **(c)** and **(d)** are from the range of 30° N to 60° N, while panels **(e)** and **(f)** show results from the tropics (30° N to 30° S).

AMTD
4, 4753–4800, 2011

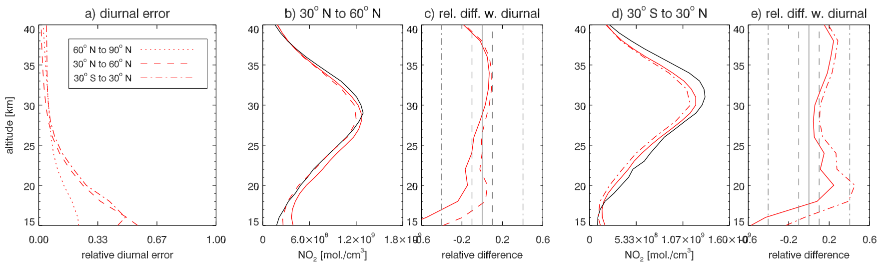

Fig. 11. **(a)** Relative diurnal effect errors for the SAGE II mean profiles shown in Fig. 10. A model was used to estimate the diurnal effect error for each SAGE II occultation. These represent the mean errors over the latitude bin. The influence of this error on the agreement between the SAGE II and SCIAMACHY is estimated in panels **(b)** and **(c)** for middle latitudes and **(d)** and **(e)** for tropics. The averaged NO_2 profiles from Fig. 10 are displayed as black (SCIAMACHY) and red solid (SAGE II) lines. The diurnally scaled mean SAGE II profile determined by removing the error from panel **(a)** is shown as red dashed line (slash-dotted for tropics). The relative difference of the mean photochemically corrected and scaled SAGE II profiles with respect to SCIAMACHY are shown in panels **(c)** and **(e)**; solid green line means without consideration of the diurnal effect and dashed line (slash-dotted for tropics) means with consideration of the diurnal effect.

AMTD
4, 4753–4800, 2011

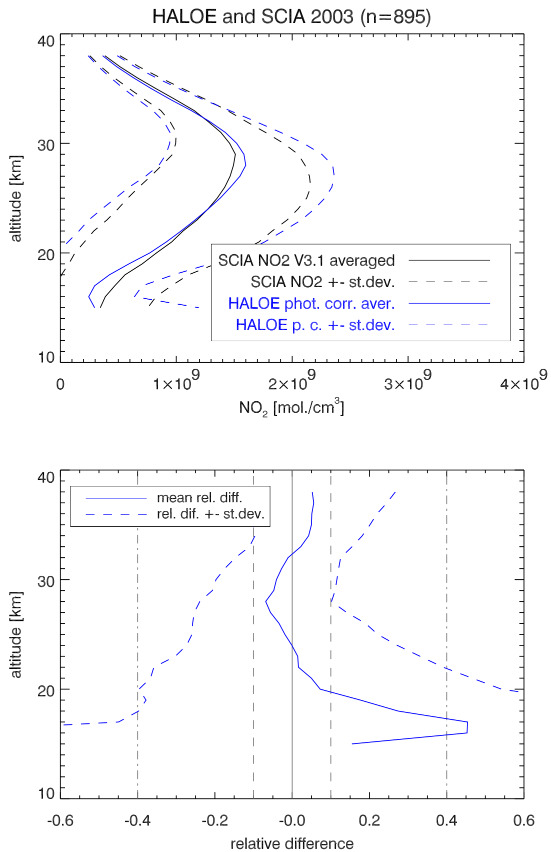

Fig. 12. For the year 2003, comparisons of HALOE NO_2 results to SCIAMACHY are shown as averaged number density profiles (number densities, upper panel) and relative deviations (lower panel).

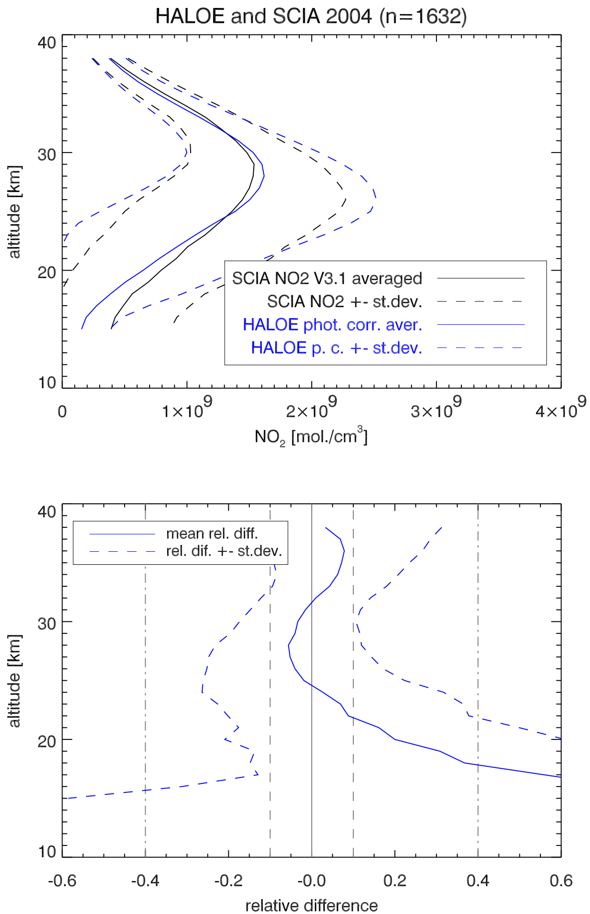

Fig. 13. Same as Fig. 12, but for 2004 data.

AMTD
4, 4753–4800, 2011

Validation of SCIAMACHY limb NO_2 profiles

R. Bauer et al.

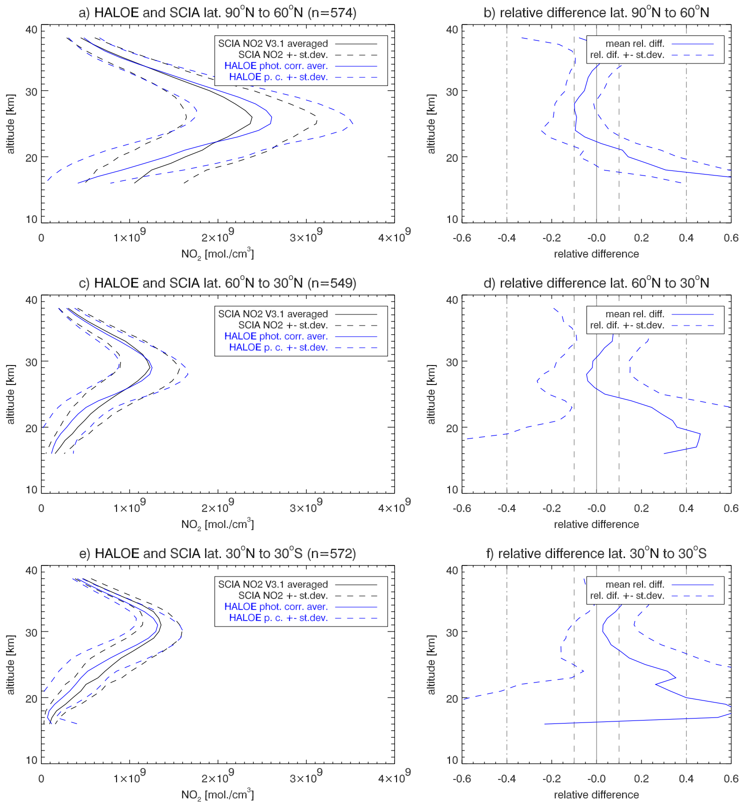

Fig. 14. Three different regions are analyzed for collocations with HALOE for the years 2003 and 2004. Panels **(a)** and **(b)**: northern latitudes (60° N to 90° N), panels **(c)** and **(d)**: mid latitudes (30° N to 60° N), panels **(e)** and **(f)**: tropics (30° N to 30° S).

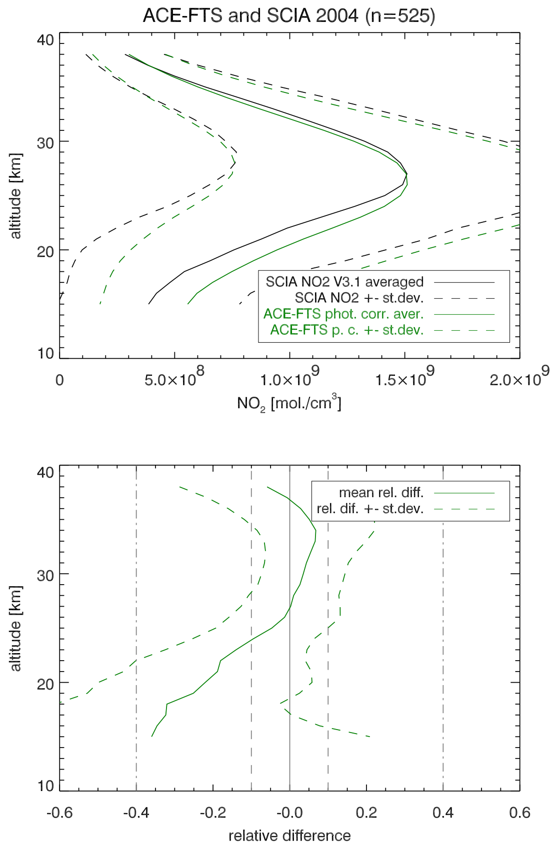

Fig. 15. Comparisons of ACE-FTS to SCIAMACHY results for the 2004 data set are shown. The upper panel shows averaged profiles, while the lower panel shows relative differences for the same data set.

AMTD
4, 4753–4800, 2011

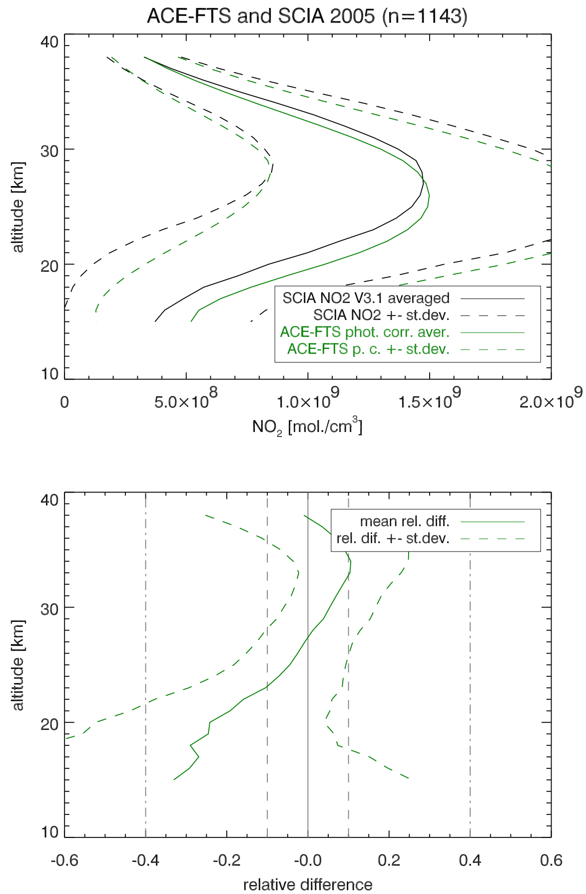

Fig. 16. Same as Fig. 15, but for 2005 data sets.

AMTD
4, 4753–4800, 2011

Validation of SCIAMACHY limb NO_2 profiles

R. Bauer et al.

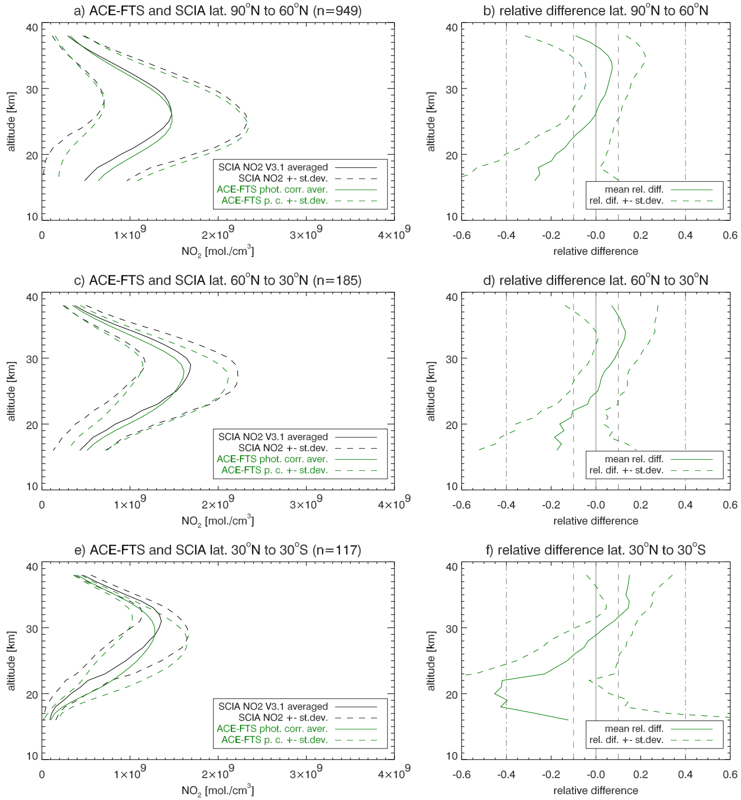

Fig. 17. Collocations for the years 2004 and 2005 are investigated for SCIAMACHY NO_2 and ACE-FTS. Panels **(a)** and **(b)**: northern latitudes (60° N to 90° N), panels **(c)** and **(d)**: middle latitudes (30° N to 60° N), panels **(e)** and **(f)**: tropics (30° N to 30° S).

AMTD
4, 4753–4800, 2011

Validation of SCIAMACHY limb NO_2 profiles

R. Bauer et al.

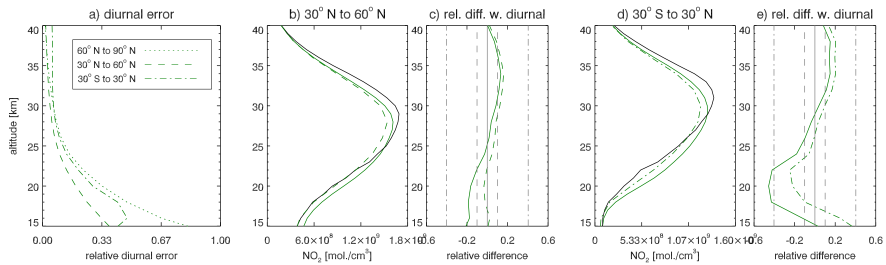

Fig. 18. For the latitude regions investigated in Fig. 17, the relative diurnal error for ACE-FTS measurements is estimated and averaged in panel **(a)**. Panel **(b)** shows an estimate of how this error influences the ACE-FTS measurements for middle latitudes. The solid black line depicts the averaged SCIAMACHY NO_2 profiles shown in panel **(c)** of Fig. 17. The solid green line shows the photochemically corrected NO2 profiles from ACE-FTS without the diurnal effect, and the green dashed line with the diurnal effect. In panels **(d)** and **(e)**, the same calculations are performed for the tropical latitudes, with the slash-dotted line marking the ACE-FTS profiles adjusted for the diurnal effect.